cyclic voltammogram of 2 in DMSO, which reveals only one quasi-reversible reduction with an $E_{1/2}$ of -0.39V vs SSCE. This wave is assigned to the IV/IV, IV/III couple and is the lowest reduction potential for a $Mn^{IV}Mn^{IV}$ dimer reported. No other redox processes are accessible within the solvent window. This potential is more than 1 V more negative than the corresponding potential for 3 (0.66V vs SCE), even though the manganese atoms in both complexes have N_2O_4 donor sets. This is indicative of the remarkable ability of Schiff base ligands, particularly the phenolate donors, to stabilize high oxidation states. This result leads us to postulate that there are probably few phenolate donors to the Mn center in the PSII OEC, because a manganese aggregate with extensive phenolate ligation would not have a sufficiently high redox potential to carry out water oxidation.

Acknowledgment. This work was supported by Grant No. GM382751 from the National Institute of General Medical Sciences. W.H.A. is grateful for a Searle Scholars Award (1986-1989). We thank Dr. Joseph Ziller at the University of California at Irvine for performing the structural studies on compound 2.

Registry No. 1, 86773-55-9; 1a, 137596-42-0; 2, 51321-10-9; 2·2DMF, 137626-07-4; 2·2DMF·H_2O, 137626-06-3.

Supplementary Material Available: Listings of hydrogen atom parameters and anisotropic thermal parameters for 1 and 2 and a complete table of interatomic angles for 2 (7 pages); listings of observed and calculated structure amplitudes for 1 and 2 (57 pages). Ordering information is given on any current masthead page.

Contribution from the Department of Chemistry, University of Michigan, Ann Arbor, Michigan 48109-1055

Manganese-Manganese Separations in Oxide- and Alkoxide-Bridged Complexes: Correlation of Structure with Ligand Type and Number

Erlund Larson, Myoung Soo Lah, Xinhua Li, Joseph A. Bonadies, and Vincent L. Pecoraro*

Received August 17, 1990

Two dimeric manganese complexes have been prepared and their structures determined using X-ray crystallography. The first is a bis(μ_2-oxo) complex {$[Mn^{IV}(SALPN)O]_2$ (1), where SALPN = 1,3-bis(salicylideneamino)propane} which had previously been reported to be an Mn(III) dimer of composition $[Mn^{III}(SALPN)(OH)]_2$. Complex 1 can be prepared by hydrogen peroxide or air oxidation of a basic solution containing $Mn^{III}(SALPN)^+$ or by the reaction of Mn(SALPN)(acac) with hydrogen peroxide. In the latter reaction, isotopic labeling studies demonstrate that both μ_2-oxo atoms of 1 are derived from the same molecule of hydrogen peroxide. The second dimer is a bis(μ_2-alkoxo) complex {$[Mn^{III}(SALAHP)Cl(CH_3OH)]_2$ (2), where $H_2SALAHP$ = 1-(salicylideneamino)-3-hydroxypropane} which is the first example of a manganese dimer with unsupported alkoxide bridges and a rare example of a chloride-containing manganese dimer. These two new dimers and twenty other manganese complexes containing μ_2-oxo and μ_2-alkoxo groups are used to develop a correlation between manganese-manganese separation and Mn-O-Mn bridge angle. It is shown that complexes containing μ-oxo bridges conform to a law of cosines correlation between Mn-Mn separations and Mn-O-Mn bridge angles. In contrast, there is marked deviation from the law of cosines behavior when μ_2-alkoxo groups form the single-atom bridge. Surprisingly, an empirical correlation with a slope of 0.03 Å/deg over a 0.95-Å range (2.86-3.81 Å) and 33° angle deviation (96-129°) is observed. Structural implications are presented for established multinuclear manganese enzymes. Crystal data are as follows. 1: monoclinic, $P2_1/c$, a = 10.827 (4) Å, b = 10.241 (4) Å, c = 17.679 (7) Å, β = 100.07 (3)°, V = 1930 (1) Å^3, Z = 2; for 2434 data collected in the range $3 < 2\theta < 45°$ and 1787 data with $I > 2\sigma(I)$ the structure refined to R = 0.068 and R_w = 0.0434. 2: monoclinic, $P2_1/c$, a = 8.428 (3) Å, b = 12.966 (3) Å, c = 12.160 (3) Å, β = 109.58 (2)°, V = 1252 (1) Å^3, Z = 2; for 1562 data collected in the range $3 < 2\theta < 45°$ and 1229 data with $I > 3\sigma(I)$ the structure refined to R = 0.034 and R_w = 0.034.

Introduction

Manganese, often in the form of dimers or higher nuclearity aggregates, plays an important role in numerous biological processes associated with the utilization or generation of hydrogen peroxide or dioxygen. At least five functions of this type are known: manganese superoxide dismutase,[1,2] manganese catalase,[3-5] manganese peroxidase,[6] manganese ribonucleotide reductase,[7] and the oxygen-evolving complex (OEC).[8] At least three of these enzymes (catalases, ribonucleotides reductase, and the oxygen-evolving complex) contain active sites composed of two or more metals.

(1) Ludwig, M. L.; Pattridge, K. A.; Stallings, W. C. *Metabolism and Enzyme Function*; Academic Press: New York, 1986; p 405.
(2) Stallings, W. C.; Pattridge, K. A.; Strong, R. K.; Ludwig, M. L. *J. Biol. Chem.* **1985**, *260*, 16424.
(3) Beyer, W. F., Jr.; Frodovich, I. *Manganese in Metabolism and Enzyme Function*; Academic Press: New York, 1986; p 193.
(4) Khangulov, S. V.; Barynin, V. V.; Melik-Adamyin, V. R.; Grebenko, A. I.; Voevodskaya, N. V.; Blumenfeld, L. A.; Dobryakov, S. N.; Il'-Yasov, V. B. *Bioorg. Khim.* **1986**, *12*, 741. Fronko, R. M.; Penner-Hahn, J. E.; Bender, C. J. *J. Am. Chem. Soc.* **1988**, *110*, 7554.
(5) Allgood, G. S.; Perry, J. J. *J. Bacteriol.* **1986**, *168*, 563.
(6) Wariishi, H.; Akileswaran, L.; Gold, M. H. *Biochemistry* **1988**, *27*, 5365. Glenn, J. K.; Akileswaran, L.; Gold, M. H. *Arch. Biochem. Biophys.* **1986**, *251*, 688.
(7) Willing, A.; Follman, H.; Auling, G. *Eur. J. Biochem.* **1988**, *170*, 603.
(8) Recent reviews discussing these points: Pecoraro, V. L. *Photochem. Photobiol.* **1988**, *48*, 249. Babcock, G. T. *Photosynthesis*; Amesz, J., Ed.; New Comprehensive Biochemistry, Vol. 15; Elsevier: Amsterdam, 1987; p 125. Asmez, J. *Biochem. Biophys. Acta* **1983**, *726*, 1. Dismukes, G. C. *Photochem. Photobiol.* **1986**, *43*, 99. Babcock, G. T.; Barry, B. A.; Debus, R. J.; Hoganson, C. W.; Atamain, M.; McIntosh, L.; Sithole, I.; Yocum, C. F. *Biochemistry* **1989**, *28*, 9557. Rutherford, A. W. *Trends Biochem. Sci.* **1989**, *14*, 227. Ghanotakis, D. F.; Yocum, C. F. *Annu. Rev. Plant Physiol. Plant Mol. Biol.* **1990**, *41*, 274. Christou, G. *Acc. Chem. Res.* **1989**, *22*, 328. Wieghardt, K. *Angew. Chem., Int. Ed. Engl.* **1990**, *28*, 1153. Govindjee; Coleman, W. J. *Sci. Am.* **1990**, *262*, 50.

0020-1669/92/1331-0373$03.00/0

X-ray absorption spectroscopy (XANES, EXAFS)[9-15] has provided detailed structural information for the lower S states[16] of the OEC. It is now established from the EXAFS that at least two of the manganese ions are separated by 2.7 Å, with longer scatters having been reported at 3.3 and 4.2 Å. In early studies, an Mn–(O,N,C) scatterer at a very short distance of ≈1.73 Å was reported. This led to the proposal[10] of a μ_2-oxo-bridged core based on the distances in the model complexes, $[Mn^{IV}O(bpy)_2]_2$ and $Mn^{IV}Mn^{III}[O(bpy)_2]_2$. Subsequent studies[12-15] have suggested that this short metal–heteroatom distance may be longer (1.78–1.91 Å). EXAFS provides information on types, numbers, and separations of scatterers, while XANES provides oxidation-state information for manganese in the OEC. However, neither region of the X-ray absorption spectrum provides angular information.

Many new types of model complexes have appeared over the past 5 years;[17-21] however, a systematic correlation among oxidation states, bridging ligand types, and metal separations has not been reported. Such a systematic study is clearly required to delineate structural possibilities in the manganese catalases, ribonucleotide reductases, and the OEC. Furthermore, if such a correlation is reliable, useful angular information can be extracted from the EXAFS-determined distances of proteins and small molecules that have not yet been analyzed successfully using X-ray crystallography. Manganese iminophenolates have modeled some of the chemistry of these manganoenzymes. Complexes that catalytically oxidize water to dioxygen when exposed to intense visible light have been reported.[22] The acidification of bis(μ-oxo)-bridged Mn(IV) iminophenolates leads to the quantitative production of hydrogen peroxide.[24] Dimers have been implicated in these model systems. In this report, we examine the relationship among oxidation states, ligand types, and metal separations in a series of manganese complexes of Schiff base and related ligands containing oxide and alkoxide bridging groups. We then examine the implications of this structural study to the manganese catalase and the oxygen-evolving complex.

Table I. Summary of Crystal Data for **1** and **2**

	1	**2**
formula	$Mn_2C_{40}H_{46}N_6O_8$	$Mn_2C_{22}H_{30}N_2O_6Cl_2$
mol wt	848.6	499.3
a, Å	10.827 (4)	8.428 (3)
b, Å	10.241 (4)	12.966 (3)
c, Å	17.679 (7)	12.160 (3)
β, deg	100.07 (3)	109.58 (2)
V, Å^3	1930 (1)	1252 (1)
cryst syst	monoclinic	monoclinic
space group	$P2_1/c$	$P2_1/c$
d_{calcd}, g/mL	1.47	1.59
d_{obsd}, g/mL	1.46 (1)	1.58 (1)
Z	2	2
radiation (λ, Å)	Mo Kα (0.7107)	Mo Kα (0.7107)
abs coeff (μ), cm^{-1}	6.53	11.8
temp, K	298	298
scan range, deg	$3 < 2\theta < 45$	$3 < 2\theta < 45$
no. of unique data collected	2434	1562
no. of obsd data ($I > 2\sigma(I)$)	1789	
no. of obsd data ($I > 3\sigma(I)$)	1287	1229
largest nonsolv residual (largest negative residual)	0.47 (0.48)	0.23 (0.24)
R	0.0680	0.034
R_w	0.0434	0.034
GOF	1.33	1.11

Experimental Section

Materials. Salicylaldehyde and 3-amino-1-propanol were obtained from Aldrich, $Mn(CH_3COO)_3 \cdot 2H_2O$ and $Mn(CH_3COO)_2 \cdot 2H_2O$ were obtained from Fluka, and hydrogen peroxide was from Malinckrodt. All other chemicals and solvents were reagent grade.

Abbreviations Used: OEC = oxygen-evolving complex; H_2SALADHP = 2-(salicylideneamino)-2-methyl-1,3-dihydroxypropane; H_2SALAHP

(9) Cole, J. L.; Yachandra, V. K.; McDermott, A. E.; Guiles, R. D.; Britt, R. D.; Dexheimer, S. L.; Sauer, K.; Klein, M. P. *Biochemistry* **1987**, *26*, 5967.

(10) Kirby, J. A.; Goodin, D. B.; Wydrzynski, T.; Robertson, A. S.; Klein, M. P. *J. Am. Chem. Soc.* **1981**, *103*, 5529.

(11) Guiles, R. D.; McDermott, A.; Yachandra, V. K.; Cole, J. L.; Dexheimer, S. L.; Britt, R. D.; Wieghardt, K.; Bossek, U.; Sauer, K.; Klein, M. P. *Biochemistry* **1990**, *29*, 471.

(12) Guiles, R. D.; Yachandra, V. K.; McDermott, A.; Cole, J. L.; Dexheimer, S. L.; Britt, R. D.; Sauer, K.; Klein, M. P. *Biochemistry* **1990**, *29*, 486.

(13) Yachandra, V. K.; Guiles, R. D.; McDermott, A.; Britt, R. D.; Dexheimer, S. L.; Sauer, K.; Klein, M. P. *Biochim. Biophys. Acta* **1986**, *850*, 324.

(14) George, G. N.; Prince, R.; Cramer, S. P. *Science* **1989**, *243*, 789.

(15) Penner-Hahn, J. E.; Fronko, R.; Pecoraro, V. L.; Bowlby, N. A.; Betts, S.; Yocum, C. F. *J. Am. Chem. Soc.* **1990**, *112*, 2549.

(16) The kinetic cycle of the oxygen-evolving complex can be described by five kinetically resolvable intermediates, termed S states, which correspond to increasingly higher oxidation levels of the enzyme. Under normal circumstances, the most reduced form of the enzyme is designated S_0 with successive oxidations labeled S_1, S_2, S_3, and S_4, respectively. Oxygen is released during the $S_3 \rightarrow S_4 \rightarrow S_0$ transition. The dark-adapted resting state is S_1.

(17) Hagen, K. S.; Armstrong, W. H.; Hope, H. *Inorg. Chem.* **1988**, *27*, 967.

(18) Vincent, J. B.; Christmas, C.; Huffman, J. C.; Christou, G.; Chang, H.-R.; Hendrickson, D. N. *J. Chem. Soc., Chem. Commun.* **1987**, 236. Christmas, C.; Vincent, J. B.; Huffman, J. C.; Christou, G.; Chang, H.-R.; Hendrickson, D. N. *J. Chem. Soc., Chem. Commun.* **1987**, 1303. Bashkin, J. S.; Chang, H.-R.; Streib, W. E.; Huffman, J. C.; Hendrickson, D. N.; Christou, G. *J. Am. Chem. Soc.* **1987**, *109*, 6502. Christou, G. *Acc. Chem. Res.* **1989**, *22*, 328.

(19) (a) Li, X.; Pecoraro, V. L. *Inorg. Chem.* **1989**, *28*, 3403. (b) Pecoraro, V. L. In *Manganese Redox Enzymes*; Pecoraro, V. L., Ed.; Verlag-Chemie: New York, in press; Chapter 13. (c) Li, X.; Lah, M. S.; Pecoraro, V. L. *Acta Crystallogr.* **1989**, *C45*, 1517. (d) Bonadies, J. A.; Kirk, M. L.; Kessissoglou, D. P.; Lah, M. S.; Hatfield, W. E.; Pecoraro, V. L. *Inorg. Chem.* **1989**, *28*, 2037. (e) Bonadies, J. A.; Maroney, M. J.; Pecoraro, V. L. *Inorg. Chem.* **1989**, *28*, 2044. (f) Kessissoglou, D. P.; Bender, C.; Kirk, M. L.; Lah, M. S.; Pecoraro, V. L. *J. Chem. Soc., Chem. Commun.* **1989**, 84. (g) Kessissoglou, D. P.; Li, X.; Kirk, M.; Pecoraro, V. L. *Inorg. Chem.* **1988**, *27*, 1. (h) Kessissoglou, D. P.; Li, X.; Butler, W. M.; Pecoraro, V. L. *Inorg. Chem.* **1987**, *26*, 2487. (i) Pecoraro, V. L.; Li, X.; Baker, M. J.; Butler, W. M.; Bonadies, J. A. *Recl. Trav. Chim. Pays-Bas* **1987**, *106*, 221. (j) Kessissoglou, D. P.; Butler, W. M.; Pecoraro, V. L. *Inorg. Chem.* **1987**, *26*, 495. (k) Pecoraro, V. L.; Kessissoglou, D. P.; Li, X.; Butler, W. M. *Prog. Photosynth. Res.* **1987**, *1*, 795. (l) Kessissoglou, D. P.; Butler, W. M.; Pecoraro, V. L. *J. Chem. Soc., Chem. Commun.* **1986**, 1253. (m) Pecoraro, V. L.; Butler, W. M. *Acta Crystallogr.* **1986**, *C42*, 1151. (n) Lah, M. S.; Pecoraro, V. L. *J. Am. Chem. Soc.* **1989**, *111*, 7258. (o) Larsen, E. L.; Haddy, A.; Kirk, M. L.; Sands, R. H.; Hatfield, W. H.; Pecoraro, V. L. Submitted for publication in *J. Am. Chem. Soc.*

(20) (a) Wieghardt, K.; Bossek, U.; Bonvoisin, J.; Beauvillain, P.; Girerd, J.-J.; Nuber, B.; Weiss, J.; Heinze, H. *Angew. Chem., Int. Ed. Engl.* **1986**, *25*, 1030. (b) Wieghardt, K.; Bossek, U.; Zsolnai, L.; Huttner, G.; Blondin, G.; Girerd, J.-H.; Babonneau, F. *J. Chem. Soc., Chem. Commun.* **1987**, 651. (c) Wieghardt, K.; Bossek, U.; Nuber, B.; Weiss, J.; Bonvoisin, J.; Corbella, M.; Vitols, S. E.; Girerd, J.-J. *J. Am. Chem. Soc.* **1988**, *110*, 7398. (d) Wieghardt, K.; Bossek, U.; Ventur, D.; Weiss, J. *J. Chem. Soc., Chem. Commun.* **1985**, 347. (e) Wieghardt, K.; Bossek, U.; Gebert, W. *Angew. Chem., Int. Ed. Engl.* **1983**, *22*, 328.

(21) (a) Sheets, J. E.; Czernuszewicz, R. S.; Dismukes, G. C.; Rheingold, A. L.; Petroleas, V.; Stubbe, J.; Armstrong, W. H.; Beer, R. H.; Lippard, S. J. *J. Am. Chem. Soc.* **1987**, *109*, 1435. (b) Goodson, P. A.; Glerup, J.; Hodgson, D. J.; Michelsen, K.; Pedersen, E. *Inorg. Chem.* **1990**, *29*, 503. (c) Mikuriya, M.; Torihara, N.; Okawa, H.; Kida, S. *Bull. Chem. Soc. Jpn.* **1981**, *54*, 1063. (d) McKee, V.; Shepard, W. B. *J. Chem. Soc., Chem. Commun.* **1985**, 158. (e) Brooker, S.; McKee, V.; Shepard, W. B.; Pannell, L. *J. Chem. Soc., Dalton Trans.* **1987**, 2555. (f) Mabad, B.; Tuchages, J.-P.; Hwang, Y. T.; Hendrickson, D. N. *J. Am. Chem. Soc.* **1985**, *107*, 2801. (g) Bhula, R.; Gainsford, G. J.; Weatherburn, D. C. *J. Am. Chem. Soc.* **1988**, *110*, 7550. (h) Diril, H.; Chang, H. R.; Zhang, X.; Potenza, J. A.; Shugar, H. A.; Hendrickson, D. N.; Isied, S. S. *J. Am. Chem. Soc.* **1987**, *109*, 2607. (i) Plaskin, P. M.; Stoufer, R. C.; Mathew, M.; Palenik, G. *J. Am. Chem. Soc.* **1972**, *94*, 2121. (j) Stebler, M.; Ludi, A.; Bürgi, H.-B. *Inorg. Chem.* **1986**, *25*, 4743.

(22) Ashmawy, F. W.; McAuliffe, C. A.; Parish, R. V.; Tames, J. *J. Chem. Soc., Dalton Trans.* **1985**, 1391.

(23) Boucher, L. J.; Coe, C. G. *Inorg. Chem.* **1975**, *14*, 1289.

(24) Evans, D. F. *J. Chem. Soc.* **1959**, 2003. Bartle, K. D.; Dale, B. J.; Jones, D. W.; Maricic, J. *J. Magn. Reson.* **1973**, *12*, 286.

Table II. Fractional Atomic Coordinates for **1**

atom	x	y	z	U, Å²
Mn1	−0.00605 (9)	0.12042 (9)	0.46636 (5)	0.0263 (3)
O1	−0.1386 (4)	0.2466 (4)	0.4399 (2)	0.030 (2)
O2	−0.0451 (4)	0.0597 (4)	0.3630 (2)	0.032 (2)
O3	−0.1088 (3)	0.0072 (4)	0.5037 (2)	0.028 (1)
O4	0.4413 (5)	0.1599 (5)	0.7785 (4)	0.083 (3)
N1	0.0371 (5)	0.2162 (5)	0.5663 (3)	0.029 (2)
N2	0.1317 (4)	0.2346 (5)	0.4327 (3)	0.030 (2)
N3	0.4289 (5)	0.0337 (6)	0.6710 (3)	0.047 (2)
C1	−0.2145 (6)	0.2816 (6)	0.4878 (4)	0.031 (3)
C2	−0.3389 (6)	0.3160 (6)	0.4593 (4)	0.035 (3)
C3	−0.4184 (6)	0.3558 (6)	0.5070 (4)	0.047 (3)
C4	−0.3768 (6)	0.3689 (7)	0.5850 (4)	0.048 (3)
C5	−0.2557 (7)	0.3372 (6)	0.6148 (4)	0.041 (3)
C6	−0.1721 (6)	0.2936 (6)	0.5685 (4)	0.029 (3)
C7	−0.0417 (6)	0.2746 (6)	0.6004 (4)	0.030 (3)
C8	0.1715 (6)	0.2242 (6)	0.5992 (4)	0.039 (3)
C9	0.2382 (6)	0.3234 (7)	0.5573 (4)	0.055 (3)
C10	0.1705 (6)	0.3551 (6)	0.4760 (4)	0.047 (3)
C11	0.1888 (6)	0.2026 (6)	0.3768 (4)	0.037 (3)
C12	0.1549 (6)	0.0944 (6)	0.3254 (3)	0.032 (3)
C13	0.2393 (6)	0.0571 (6)	0.2766 (4)	0.038 (3)
C14	0.2106 (8)	−0.0397 (7)	0.2249 (4)	0.053 (3)
C15	0.0940 (8)	−0.0998 (7)	0.2163 (4)	0.049 (3)
C16	0.0088 (6)	−0.0645 (6)	0.2618 (4)	0.037 (3)
C17	0.0383 (6)	0.0295 (6)	0.3198 (4)	0.032 (3)
C18	0.4683 (7)	0.1366 (8)	0.7156 (5)	0.065 (4)
C19	0.4674 (7)	0.0136 (8)	0.5965 (4)	0.073 (4)
C20	0.3486 (7)	−0.0638 (7)	0.6978 (4)	0.065 (3)

= 3-(salicylideneamino)-1-hydroxypropane; H_2SALPN = 1,3-bis(salicylideneamino)propane; H_2SALEN = 1,2-bis(salicylideneamino)ethane; H_2(2-OH-(5-Cl-SAL)PN) = 1,3-bis(5-chlorosalicylideneamino)-2-hydroxypropane; H_2(2-OH-SALPN) = 1,3-bis(salicylideneamino)-2-hydroxypropane; TACN = 1,4,7-triazacyclononane; Me_3TACN = 1,4,7-trimethyl-1,4,7-triazacyclononane; phen = phenanthroline; bispicen = *N*,*N*′-bis(2-pyridylmethyl)-1,2-ethanediamine; H(pz)$_3$B = hydrotris(1-pyrazolyl)borate; H_3tren = tris(2-hydroxyethyl)amine.

Preparation of Compounds. **[$Mn^{IV}(\mu_2$-O)(SALPN)]$_2$·2DMF (1).** The ligand SALPN (2.82 g, 10 mmol) was dissolved in 250 mL of methanol with no effort to exclude dioxygen or water. To this was added 4 equiv of NaOH pellets. The resulting yellow solution was warmed to dissolve the base completely. At this point, $Mn(OAc)_3·2H_2O$ (10 mmol) was added and air bubbled through the resultant dark brown solution for 4 h. A dark red microcrystalline solid (**1**) was obtained upon suction filtration. The yield was >90%. The solid was redissolved in DMF, and X-ray-quality crystals were recovered by slow evaporation at room temperature. Anal. Calcd for $Mn_2C_{40}H_{46}N_6O_8$ (mol wt 848.6): C, 56.56; H, 5.42; N, 9.90; Mn, 13.0. Found: C, 56.45; H, 5.24; N, 9.56; Mn, 13.31.

[Mn^{III}(SALAHP)Cl(CH_3OH)]$_2$ (2). A deep green solution of **2** was generated by the addition of $MnCl_2·4H_2O$ (7.44 g, 37.6 mmol) to a solution of salicylaldehyde (2 mL, 18.8 mmol) and 3-amino-1-propanol (1.45 mL, 18.8 mmol) in methanol. After 5 h of reflux, the solution volume was reduced to 75% by evaporation of the solvent on a Schlenk line. Green prismatic crystals were obtained after the solution was left to stand overnight. Overall yield: 70%. Anal. Calcd for $Mn_2C_{22}H_{30}N_2O_6Cl_2$ (mol wt 599.3): C, 44.05; H, 5.01; N, 4.67; Mn, 18.35; Cl, 11.83. Found: C, 43.70; H, 5.14; N, 4.58; Mn, 18.47; Cl, 11.70.

Methods. Infrared spectra were recorded on a Nicolet 60 SX Fourier transform spectrometer with samples prepared as KBr pellets. Solid-state magnetic susceptibilities were determined using a Johnson-Mathey magnetic susceptibility balance [MSB-1] and Hg[Co(SCN)$_4$] as a standard. Solution magnetic susceptibilities were determined by the Evans method[24] using a 360-MHz Bruker FT-NMR spectrometer. UV/vis spectra were recorded on a Perkin-Elmer Lambda 9 UV/vis/near-IR spectrophotometer equipped with a Perkin-Elmer 3600 data station.

Collection and Reduction of X-ray Data. Suitable crystals of **1** and **2** were obtained as described above. Each crystal was then mounted in a glass capillary, and data were collected on a Syntex P2$_1$ diffractometer. Intensity data were obtained using Mo Kα radiation (λ 0.7107 Å) monochromatized from a graphite crystal whose diffraction vector was parallel to the diffraction vector of the sample. Three standard reflections were measured every 97 reflections. Lattice parameters were determined from a least-squares refinement of 15 reflection settings obtained from an automatic centering routine. Table I contains a summary of data collection conditions and results for each structure.[25] The data were reduced by using the SHELX76 program package, and the structure was solved using SHELX86. In the subsequent refinement, the function $\sum w(|F_o| - |F_c|)^2$ was minimized where $|F_o|$ and $|F_c|$ are the observed and calculated structure factor amplitudes. The agreement indices $R = \sum||F_o| - |F_c||/|F_o|$ and $R_w = [\sum w(|F_o| - |F_c|)^2/\sum w|F_o|^2]^{1/2}$ were used to evaluate the results. Atomic scattering factors are from ref 26. Absorption corrections were not applied. Hydrogen atoms were placed at fixed distances from bonded carbon atoms of 0.96 Å in the final least-squares refinement. Hydrogen atom isotropic temperature factors were allowed to refine using a riding model with separate free variables defined for methyl, methylene, and aromatic hydrogens. Tables II and III provide

Table III. Fractional Atomic Coordinates for **2**

atom	x	y	z	U, Å²
Mn1	0.9563 (1)	0.9790 (1)	0.1082 (1)	0.031
Cl1	1.1392 (2)	1.1227 (1)	0.2275 (1)	0.044
O1	0.7711 (4)	1.0152 (3)	0.1490 (3)	0.043
O2	1.1219 (4)	0.9428 (2)	0.0376 (3)	0.034
O3	0.8141 (5)	0.8358 (3)	0.0081 (3)	0.052
N1	1.0380 (5)	0.8793 (3)	0.2403 (3)	0.035
C1	0.7542 (6)	1.0086 (4)	0.2542 (4)	0.033
C2	0.6324 (6)	1.0695 (4)	0.2768 (4)	0.041
C3	0.6092 (7)	1.0640 (4)	0.3842 (4)	0.049
C4	0.7034 (7)	0.9973 (4)	0.4702 (4)	0.049
C5	0.8229 (6)	0.9367 (4)	0.4488 (4)	0.043
C6	0.8514 (6)	0.9405 (4)	0.3411 (4)	0.035
C7	0.9809 (6)	0.8762 (4)	0.3259 (4)	0.036
C8	1.1677 (7)	0.8034 (4)	0.2374 (4)	0.046
C9	1.3114 (6)	0.8552 (4)	0.2073 (4)	0.042
C10	1.2542 (7)	0.8797 (4)	0.0788 (4)	0.048
C11	0.6577 (7)	0.8013 (5)	0.0145 (5)	0.056

Table IV. Selected Bond Lengths (Å) and Angles (deg) for **1**

Mn1–Mn1′	2.731 (2)	Mn1–O3	1.810 (4)
Mn1–O1	1.927 (4)	Mn1–N1	2.003 (4)
Mn1–O2	1.906 (3)	Mn1–N2	2.063 (5)
O1–Mn1–O2	87.4 (2)	O2–Mn1–N2	87.7 (2)
O1–Mn1–O3	92.3 (2)	O3–Mn1–N1	93.2 (2)
O1–Mn1–N1	86.3 (2)	O3–Mn1–N2	171.8 (2)
O1–Mn1–N2	95.5 (2)	N1–Mn1–N2	84.7 (2)
O2–Mn1–O3	95.4 (2)	Mn1–O3–Mn1	97.7 (3)
O2–Mn1–N1	169.6 (2)		

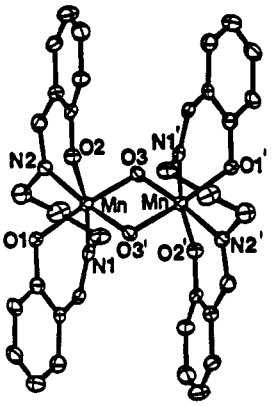

Figure 1. ORTEP diagram of [Mn^{IV}(SALPN)O]$_2$ (**1**), showing the atom-numbering scheme and thermal ellipsoids at 30% probability.

(25) Computations were carried out on an Amdahl 5860 computer. Computer programs used during the structural analysis were from the SHELX program package by George Sheldrick, Institut für anorganische Chemie der Universität Göttingen, Federal Republic of Germany. Other programs used included ORTEP, a thermal ellipsoidal drawing program by C. K. Johnson, and the direct-methods program MULTAN78 by Peter Main.

(26) *International Tables for X-Ray Crystallography*, Ibers, J. A., Hamilton, W. C., Eds.; Kynoch Press: Birmingham, England, 1974; Vol. IV, Tables 2.2 and 2.3.1.

(27) Maslen, H. S.; Waters, T. N. *J. Chem. Soc., Chem. Commun.* **1973**, 760.

(28) Gohdes, J. W.; Armstrong, W. A. *Inorg. Chem.*, preceding paper in this issue.

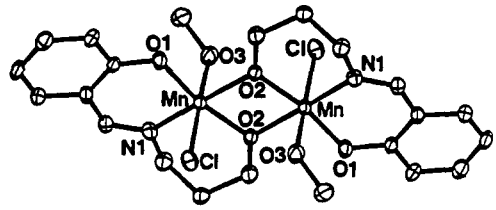

Figure 2. ORTEP diagram of $[Mn^{III}Cl(SALAHP)(CH_3OH)]_2$ (**2**), showing the atom-numbering scheme and thermal ellipsoids at 30% probability.

vide fractional atomic coordinates for **1** and **2**, respectively.

Results and Discussion

Description of Structures. $[Mn(SALPN)O]_2$ Complexes. A partial description of the structure of **1** as the tetrapyridine solvate has appeared,[29] although the Mn ions were erroneously assigned to the +3 oxidation level and the bridging oxygen atoms were described as μ_2-OH moieties. Unfortunately, neither an *R* value nor goodness-of-fit criterion was provided in the previous communication. Also, the Mn–Mn separation (2.72 Å) was the only quantitative piece of structural data provided. For these reasons, we have recollected the data and solved the structures of what are actually dinuclear Mn(IV) species, $[Mn(SALPN)O]_2$, and report the complete crystallographic and structural parameters for this important molecule in Tables I, II, and IV. A contemporaneous structural determination can be found in the preceding paper.[28] An ORTEP diagram is provided in Figure 1.

That **1** is an Mn(IV), not Mn(III), complex is demonstrated in numerous ways. First, the compound shows only reductive electrochemistry (confirmed using rotating platinum electrode voltammetry)[29] which generates mononuclear Mn(III) compounds that have been extensively characterized by us[19d,e,30] and others.[23] Second, redox titration to form Mn(II) yields four electrons per dimer. Third, an authentic[30] Mn(III) dimer, $[Mn^{III}(SALPN)(CH_3O)]_2$, has electronic, electrochemical, and magnetic properties that are significantly different from those of **1**.

$[Mn^{III}(SALAHP)Cl(CH_3OH)]_2$ (2). We[19c,f-j] and others[31] have shown the utility of using hydroxyl-rich Schiff base ligands such as SALAHP and SALADHP (SALA series) to form dimeric and trimeric manganese(III) materials. The meridional, tridentate chelation mode using phenolate and alkoxide oxygens and imine nitrogen atoms of the SALA series of ligands has been well documented for manganese and vanadium complexes. A dinuclear complex, $[Mn^{III}(SALAHP)(CH_3CO_2)]_2$ (**3**), containing two trans,syn-acetato and two μ_2-alkoxide bridges has appeared.[31] Additionally, linear and bent mixed-valent trinuclear complexes, such as $Mn_3(SALADHP)_2(CH_3CO_2)_4(CH_3OH)_2$ (**4**), with two cis,syn-acetato and one μ_2-alkoxide bridges linking Mn(III) and Mn(II) ions are known.[19f,g] Unsupported bis(μ_2-alkoxide) bridges between vanadium(IV) atoms, $[V^{IV}O(SALAHE)]_2$, are now reported.[32] However, complex **2**, illustrated in Figure 2, represents the first example of this molecular class to contain two unsupported μ_2-alkoxide bridges between manganese atoms. Important bond lengths and angles for **2** and **3** are provided for comparison in Table V. While the Mn1–O2–Mn1′–O2′ atoms in **2** are strictly planar with an anti orientation of bound chloride and methanol, $[V^{IV}O(SALAHE)]_2$ is five-coordinate,[32] has two syn terminal oxo groups, and forms a bent V1–O2–V1′–O2′ core.

Table V. Selected Bond Lengths (Å) and Angles (deg) for **2** and the Comparison with **3**[31]

	Complex **2**		
Mn1–Mn1′	3.011 (1)	Mn1–O1	1.850 (3)
Mn1–O2	1.926 (3)	Mn1–O2′	1.955 (4)
Mn1–O3	2.321 (4)	Mn1–N1	1.995 (4)
Mn1–Cl1	2.541 (1)		
Cl1–Mn1–O1	93.8 (1)	Cl1–Mn1–O2	92.4 (1)
Cl1–Mn1–O3	173.8 (1)	O1–Mn1–O2	169.8 (1)
O1–Mn1–O3	90.6 (1)	O2–Mn1–O3	84.0 (1)
Cl1–Mn1–N1	92.1 (1)	O1–Mn1–N1	92.5 (1)
O2–Mn1–N1	95.5 (1)	O3–Mn1–N1	83.3 (1)
O2–Mn1–O2′	78.2 (1)	Mn1–O2–Mn1′	101.8 (1)
	Complex **3**		
Mn1–Mn1′	2.869 (1)	Mn1–O1	1.849 (2)
Mn1–O2	1.899 (2)	Mn1–O2′	1.951 (2)
Mn1–O3	2.251 (2)	Mn1–N1	2.006 (2)
Mn1–O4	2.208 (2)	Mn1–O2–Mn1′	96.34 (8)

As discussed in more detail below, one sees a smooth trend for the increase in metal–metal separation and Mn–O–Mn bridge angle as bridging acetate groups are replaced by monodentate, nonbridging ligands. Substitution of methanol and chloride for acetate on the $[Mn^{III}(SALAHP)]_2^{2+}$ core leads to a marked increase in the manganese manganese separation (**2**, 3.011 Å; **3**, 2.86 Å) and to an expansion of the Mn1–O–Mn1′ bond angles (**2**, 101.8°; **3**, 96.3°). The related complex[33] $Mn^{III}_2[(\mu_2\text{-2-alkoxy-SALPN})(\mu_2\text{-}CH_3O)(CH_3OH)(acetate)]$ (**5**), with a dialkoxy, monoacetato bridging core has intermediate structural parameters (Mn–Mn = 2.93 Å; Mn–O–Mn(av) = 98°). These distances and angles are significantly compressed compared to those of single-alkoxide-bridged complexes such as **4** (described above; Mn–Mn = 3.51 Å; Mn–O–Mn(av) = 120°) and $[Mn^{III}(2\text{-OH-SALPN})(CH_3OH)_{0.5}]_2$ (**6**), which has an unsupported alkoxide bridge (Mn–Mn = 3.81 Å; Mn–O–Mn(av) = 129°).

Another interesting feature of **2** is that it is a rare example of a dimeric manganese cluster with a monodentate Mn–Cl bond. It is now recognized that chloride can act as a competitive inhibitor of the manganese catalase, presumably by binding to the dinuclear metal center of this enzyme.[34] Furthermore, chloride is an important cofactor of the photosynthetic water-oxidizing reaction[35] and has been proposed to bind to the manganese atoms of this enzyme. Complex **2** illustrates how chloride could occupy a syn position to a coordinated substrate and possibly block subsequent nonproductive oxidation reactions[36] in the lower S states of this enzyme.

Distance and Angle Correlation. The correlation between Mn–Mn separation and Mn–O–Mn angle for 22 complexes[37] is shown in Figure 3, and the data are compiled in Table VI. This correlation is based on crystallographically determined structures

(29) Rotating platinum electrode (RPE) voltammetry samples the properties of the bulk solution, since the product of the electrode reaction is continuously swept away. This allows one to establish whether an oxidative or reductive current is passed. In contrast, cyclic voltammetry samples the electroactive species at the electrode surface and does not distinguish a priori whether the original state of the electroactive component is oxidized or reduced. For more details see: Bard, A. J.; Faulkner, L. R. *Electrochemical Methods: Fundamentals and Applications*; John Wiley & Sons: New York, 1980.

(30) Larson, E. L.; Pecoraro, V. L. *J. Am. Chem. Soc.* **1991**, *113*, 3810.

(31) Mikuriya, M.; Torihara, N.; Okawa, H.; Kida, S. *Bull. Chem. Soc. Jpn.* **1981**, *54*, 1063.

(32) Carrano, C. J.; Nunn, C.; Quan, R.; Bonadies, J. A.; Pecoraro, V. L. *Inorg. Chem.* **1990**, *29*, 944.

(33) Nishida, Y.; Oshino, N.; Tokii, T. *Z. Naturforsch.* **1988**, *43B*, 472.

(34) Penner-Hahn, J. E. In *Manganese Redox Enzymes*; Pecoraro, V. L., Ed.; Springer-Verlag: New York, 1991.

(35) Yocum, C. F. In *Manganese Redox Enzymes*; Pecoraro, V. L., Ed.; Springer-Verlag: New York, 1991.

(36) Frasch, W.; Mei, R. *Biochemistry* **1987**, *26*, 7321. Mano, J.; Takahashi, M.; Asada, K. *Biochemistry* **1987**, *26*, 2495.

(37) Numbering scheme used in Table VI: **1** = $[Mn^{IV}(SALPN)O]_2$; **2** = $[Mn^{III}(SALAHP)Cl(CH_3OH)]_2$; **3** = $[Mn^{III}(SALAHP)(CH_3CO_2)]_2$; **4** = β-$Mn^{II}Mn^{III}_2(SALADHP)_2(CH_3CO_2)_4(CH_3OH)_2$; **5** = $Mn^{III}_2[(\mu_2\text{-2-alkoxy-SALPN})(\mu_2\text{-}CH_3O)(CH_3OH)(acetate)]$; **6** = $[Mn^{III}(2\text{-OH-SALPN})(CH_3OH)_{0.5}]_2$; **8** = $[Mn^{III}(5\text{-Cl-SALPN})(CH_3O)]_2$; **9** = $[Mn^{IV}O_{1.5}(Me_3TACN)]_2$; **10** = $[Mn^{IV}O_{1.5}(TACN)]_4Br_4$; **11** = $[Mn^{IV}(phen)O_2]_2(ClO_4)_4$; **12** = $\{Mn^{III}Mn^{IV}[(phen)O]_2\}(PF_6)_3$; **13** = $[Mn^{IV}(bispicen)O]_2$; **14** = $\{Mn^{III}Mn^{IV}[(TACN)_2O_2(CH_3CO_2)]\}^{2+}$; **15** = $\{Mn^{III}Mn^{IV}[(tren)O]_2\}$; **16** = $[Mn^{IV}(TACN)O(OH)]_2^{2+}$; **17** = $\{Mn^{III}Mn^{IV}[(TACN)O_{0.5}(CH_3CO_2)]_2\}$; **18** = $[Mn^{III}(TACN)O_{0.5}(CH_3CO_2)]_2$; **19** = $[Mn^{III}(H(pz)_3B)O_{0.5}(CH_3CO_2)]_2$; **20** = α-$Mn^{II}Mn^{III}_2(SALADHP)_2(CH_3CO_2)_4(CH_3OH)_2$; **21** = $Mn_2O(5\text{-}NO_2saldien)_2$; **22** = $[Mn_4O_2(TPHPN)_2(H_2O)_2(CF_3SO_3)_3]^{3+}$; **23** = $[Mn^{II}Mn^{III}_3(\mu_2\text{-O})(\mu_2\text{-OH})(acetate)_2(1,3\text{-diamino-2-hydroxypropane-}N,N,N',N'\text{-tetraacetate(3-)})_2]$; **24** = $[Mn^{III}Mn^{IV}(2\text{-OH-SALPN})_2(THF)]^+$.

(38) Stibrany, R. T.; Gorun, S. M. *Angew. Chem., Int. Ed. Engl.* **1990**, *29*, 1156.

Table VI. Correlation among Metal Oxidation State, Distance, and Bridging Ligand for Manganese Complexes[37]

complex	oxidn state	dist, Å		angle, deg	bridging ligand		ref
		M–M	M–O	M–O–M	type[a]	no.	
9	Mn(IV/IV)	2.296	1.82	78	O	3	20c
1	Mn(IV/IV)	2.719	1.81	98	O	2	this work
10	Mn(IV/IV)	3.21	1.79	127.3	O[b]	1.5[b]	20c,e
11	Mn(IV/IV)	2.748	1.80	99.5	O	2	21j
12	Mn(IV/III)	2.716	1.78,[c] 1.85[d]	96.6	O	2	21j
13	Mn(IV/IV)	2.672	1.81	95.0	O	2	21b
14	Mn(IV/III)	2.588	1.81	91.1	O, A	2, 1	20b
15	Mn(IV/III)	2.679	1.77,[c] 1.85[d]	95.3	O	2	17
16	Mn(IV/IV)	2.625	1.82	91.9	O	2	20c
3	Mn(III/III)	2.869	1.93	96.3	Alk, A	2, 2	33
2	Mn(III/III)	3.011	1.94	101.8	Alk	2	this work
8	Mn(III/III)	3.19	1.90, 2.22[e]	101.3	Alk	2	30
17	Mn(IV/III)	3.230	1.81,[b] 1.83[c]	125.1	O, A	1,2	20a
18	Mn(III/III)	3.084	1.80	117.8	O, A	1,2	20d
19	Mn(III/III)	3.159	1.78	125.1	O, A	1, 2	21a
5	Mn(III/III)	2.93	1.95	98	Alk, A	2, 1	33
6	Mn(III/III)	3.81	2.32,[e] 1.90	128.9	Alk	1	19d
4	Mn(III/II)	3.50	1.88,[d] 2.17[f]	119.6	Alk, A	1, 2	19f
20	Mn(III/II)	3.55	1.89,[d] 2.14[f]	121.7	Alk, A	1, 2	19g
21	Mn(III/III)	3.49	1.75	168.4	O	1	19b
22[g]	Mn(III/II)	3.38	1.82	136.8	O, A	1, 1	36
		3.72	1.95	132.5	Alk	1	
23[h]	Mn(III/IV)	2.72	1.82	96.0	O	2	19c
23[h]	Mn(II/III–IV)	3.87	1.94, 2.23	136.9	Alk	1	19c
24	Mn(III/IV)	3.65	1.89, 2.20	126.7	Alk	1	19o

[a] Abbreviations: O = oxide, Alk = alkoxide, A = acetate. [b] This is a tetranuclear adamantane cluster and as such has the Mn(IV)–Mn(IV) separation of interest supported by what could be considered two (O–Mn(IV)–O) bridges. [c] Mn(IV)–O distance. [d] Mn(III)–O distance, non-Jahn–Teller axis. [e] Mn(III)–O distance, Jahn–Teller axis. [f] Mn(IV)–O distance. [g] This tetranuclear complex also contains an Mn–Mn separation of 3.58 Å across an angle of 137.2°. We have not included this on the chart, since it represents the equivalent of a μ_2-OH bridge rather than an oxide or alkoxide ligand. [h] This tetranuclear complex contains a mixed-valence $(\mu_2\text{-O})_2\text{Mn}^{\text{III/IV}}$ pair (2.72 Å) with both manganese linked to Mn(II) ions by a single alkoxide. The Mn(III/IV) pair is reminiscent of compounds **12**, **14**, and **15**, while the single-alkoxide bridge is similar to that in compounds **5** and **6**.

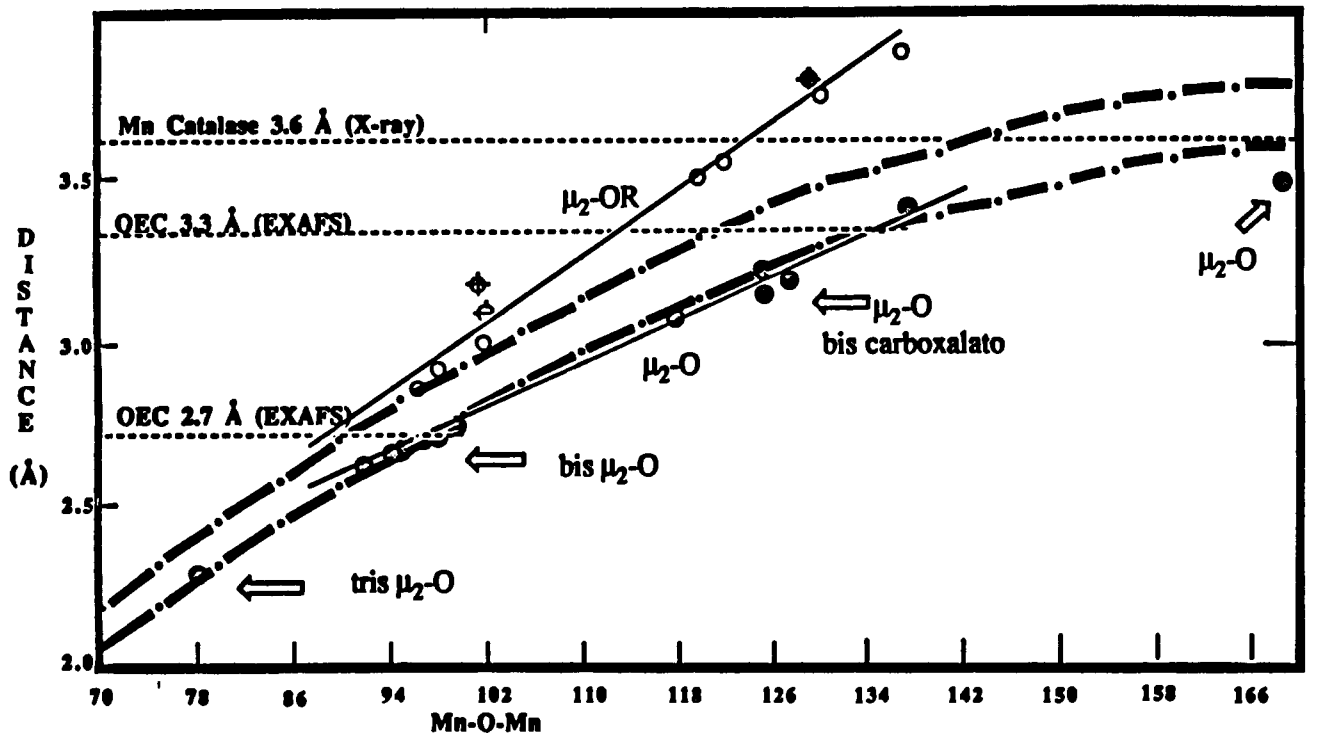

Figure 3. Correlation between Mn–Mn distance and Mn–O–Mn bridging angle for 23 crystallographically characterized compounds containing μ_2-oxo or μ_2-alkoxo bridges. The slope of the line for the oxo complexes is 0.02 Å/deg and for alkoxo complexes is 0.03 Å/deg. See ref 37 for identification of compounds and text for discussion of implications of these data.

of Mn(II/III), Mn(III/III), Mn(III/IV), and Mn(IV/IV) complexes with μ_2-oxide, μ_2-alkoxide, and μ_2-acetate bridges. The metal separations span 1.6 Å (2.296–3.874 Å), and the Mn–O–Mn angles range over 90° (78–168°). Complexes with at least one μ-oxo bridge fall on one curve (bottom heavy dot–dash curve in Figure 3) calculated assuming the law of cosines and a fixed Mn–O distance of 1.8 Å. The excellent fit is oxidation state independent. The bottom solid line (Figure 3) demonstrates that one can approximate the Mn–Mn separation vs Mn–O–Mn angle by a nearly linear relationship between 90 and 130°.

This correlation breaks down for alkoxide bridges as a result of two factors, the orientation of the Jahn–Teller distortion axis

and the relative destabilization of higher oxidation states using alkoxide versus oxide ligands. The top heavy dashed curve (Figure 3) shows the predicted angular dependence with a fixed Mn–μ_2-OR distance of 1.9 Å. Only three compounds, with Jahn–Teller distortions for manganese ions oriented perpendicular to the (Mn–μ_2-OR) plane, fall on this curve. This emphasizes the necessity of using the cosine law curve for Mn(III) compounds that have the Jahn–Teller distortion perpendicular to the Mn–(bridging heteroatom) axis. Surprisingly, the Mn(III/III) and Mn(III/II) alkoxide compounds exhibit a linear trend from 94 to 134° and from 2.9 to 3.8 Å (top solid line in Figure 3).[39] Therefore, one can use this empirical observation to predict the Mn–(μ_2-OR)–Mn angle when metal separations (derived from EXAFS) and chemical composition are known.

Dimers with μ_2-O^{2-} bridges closely follow the cosine curve because the bridge is strongly basic. These molecules have Jahn–Teller distortions perpendicular to $[Mn(\mu_2\text{-}O)]_2$. Furthermore, μ_2-O^{2-} bridges stabilize the Mn(III) and Mn(IV) oxidation levels. In contrast, the less basic alkoxides are less able to define either the oxidation level of the manganese or the orientation of the Jahn–Teller axis of Mn(III). This leads to marked deviations from the simple cosine treatment. Fortunately, a linear trend is apparent for the alkoxides. We conclude that structural predictions for Mn(μ_2-O) compounds can be made with great reliability regardless of oxidation state and that reasonably reliable angles can be extracted for alkoxide complexes as long as one of the manganese ions is in the +3 or +4 oxidation state.

In addition to elaborating possible structural predictions for manganese compounds, this data treatment can cautiously be used to extract the following implications for the active-site structure of manganese enzymes. If the active site of the OEC contains a dimer of dimers, the most likely bridging form, based on the 2.7-Å Mn–Mn distance observed in the EXAFS of S_1 and S_2, is a bis(μ-oxo) (such as in **1**) or acetato/bis(μ-oxo) bridged species with Mn–O–Mn angles between 95 and 100°. This conclusion is qualitatively identical to that previously suggested by numerous other workers in this field;[8-13,18-21] however, it places relatively rigorous quantitative constraints on these models. It is highly unlikely that alkoxide bridges will lead to this short metal–metal separation. Either a diacetato/μ-oxo bridge or alkoxo bridges (e.g., $[Mn^{III}(SALPN)(CH_3O)]_2$) could lead to the Mn–Mn scatterer at 3.3 Å. A μ-OH bridge cannot be excluded, since there are few structural data on this bridging type.

While the analysis given above is merely fine tuning of previous structural proposals for the manganese cluster in the oxygen-evolving complex, systems that have had lesser attention are the *T. thermophilus* and *L. plantarum* manganese catalases. A low-resolution X-ray structure[40] of the *T. thermophilus* enzyme shows a Mn–Mn separation of 3.6 Å. The correlation data in Figure 3 provide the following prediction for the manganese cluster *if* the crystallographically determined distance is corrected. The metals in the crystallized form may be bridged by a μ-hydroxo group or a protein-based ligand such as threonine, serine, or tyrosine rather than a μ-oxo moiety (only a linear μ_2-O could satisfy the Mn–Mn separation restriction). The single-atom-bridge angle of this dimer is probably in the range 120–135°. These conclusions are consistent with the recent assertion that the Mn catalase has a low-valent catalytic cycle which, most likely, utilizes Mn(II/II) and Mn(III/III) forms.[34]

Acknowledgment. We wish to thank Professors W. Armstrong, G. T. Babcock, G. Brudvig, W. Frasch, M. Klein, J. Penner-Hahn, K. Sauer, R. Sharp, T. Vänngard, and C. F. Yocum for insightful discussions and access to manuscripts from their laboratories prior to publication. V.L.P. thanks the G. D. Searle Family/Chicago Community Trust for Biomedical Research Scholar's Awards (1986–1989) and the Alfred P. Sloan Foundation for a fellowship. This work was supported by NIH Grant GM 39406.

Registry No. **1**, 137626-07-4; **2**, 137596-24-8; salicylaldehyde, 90-02-8; 3-amino-1-propanol, 156-87-6.

Supplementary Material Available: For **1** and **2**, tables of anisotropic thermal parameters, fractional atomic positions for hydrogen atoms, and complete bond distances and angles and figures providing complete numbering schemes (11 pages); listings of observed and calculated structure factors (15 pages). Ordering information is given on any current masthead page.

(39) The apparent one to one correspondence results from the variable length of the Mn–OR bond for Mn(III) in the tetragonal plane (≈1.9 Å) or Jahn–Teller axis (≈2.1 Å) or for Mn(II) (≈2.2 Å). Thus, the alkoxide complexes really are located on three separate law of cosine curves that represent combinations of these possibilities (1.9 and 1.9 Å; 1.9 and 2.1 Å; or 1.9 and 2.2 Å). When the alkoxides are the strongest bases in the complex (those with shortest Mn–Mn separation), they define the Jahn–Teller axis perpendicular to the plane. When other ligands are equally or more basic, the Jahn–Teller axis is along the bridge, leading to a longer Mn–Mn separation. If the other ligands are not sufficiently basic, the Mn(III) oxidation level is destabilized and Mn(II) with longer bonds is recovered. Fortuitously, the known molecules cluster in regions on each cosine curve which can be represented remarkably well by a straight line.

(40) Barynin, V. V.; Vagin, A. A.; Melik-Adamyin, V. R.; Grebenko, A. I.; Khangulov, S. V.; Popov, A. N.; Anrianova, M. E.; Vainshtein, B. K. *Sov. Phys.—Dokl. (Engl. Transl.)* **1986**, *31*, 457.